Basic Science and Experimental Studies

Effects of an Interatrial Shunt on Rest and Exercise Hemodynamics: Results of a Computer Simulation in Heart Failure

DAVID KAYE, MD, PhD,[1] SANJIV J. SHAH, MD,[2] BARRY A. BORLAUG, MD,[3] FINN GUSTAFSSON, MD,[4] JAN KOMTEBEDDE, DVM,[5] SPENCER KUBO, MD,[6] CHRIS MAGNIN,[5] MATHEW S. MAURER, MD,[7] TED FELDMAN, MD,[8] AND DANIEL BURKHOFF, MD, PhD[7]

Melbourne, Australia; Chicago and Evanston, Illinois; Rochester and Minneapolis, Minnesota; Copenhagen, Denmark; Boston, Massachusetts; and New York, New York

ABSTRACT

Background: A treatment based on an interatrial shunt device has been proposed for counteracting elevated pulmonary capillary wedge pressure (PCWP) in patients with heart failure and mildly reduced or preserved ejection fraction (HFpEF). We tested the theoretical hemodynamic effects of this approach with the use of a previously validated cardiovascular simulation.

Methods and Results: Rest and exercise hemodynamics data from 2 previous independent studies of patients with HFpEF were simulated. The theoretical effects of a shunt between the right and left atria (diameter up to 12 mm) were determined. The interatrial shunt lowered PCWP by ~3 mm Hg under simulated resting conditions (from 10 to 7 mm Hg) and by ~11 mm Hg under simulated peak exercise conditions (from 28 to 17 mm Hg). Left ventricular cardiac output decreased ~0.5 L/min at rest and ~1.3 L/min at peak exercise, with corresponding increases in right ventricular cardiac output. However, because of the reductions in PCWP, right atrial and pulmonary artery pressures did not increase. A majority of these effects were achieved with a shunt diameter of 8−9 mm. The direction of flow though the shunt was left to right in all of the conditions tested.

Conclusions: The interatrial shunt reduced left-sided cardiac output with a marked reduction in PCWP. This approach may reduce the propensity for heart failure exacerbations and allow patients to exercise longer, thus attaining higher heart rates and cardiac outputs with the shunt compared with no shunt. These results support clinical investigation of this approach and point out key factors necessary to evaluate its safety and hemodynamic effectiveness. (*J Cardiac Fail 2014;20:212−221*)

Key Words: Left atrial pressure, heart failure, diastolic dysfunction, heart failure with preserved ejection fraction, interatrial shunt, computer simulation.

Development of treatments for patients with heart failure and preserved ejection fraction (HFpEF) or mildly reduced ejection fraction is among the highest priority in cardiology today. These patients represent >50% of all patients with heart failure (HF) and experience rates of morbidity and mortality that are similar to patients with HF and reduced ejection fraction.[1−3] To date, there are no therapies that are proven to be effective in these patients. This could be

From the [1]Baker IDI Heart and Diabetes Institute and Alfred Hospital, Melbourne, Australia; [2]Division of Cardiology, Department of Medicine, Northwestern University Feinberg School of Medicine, Chicago, Illinois; [3]Division of Cardiovascular Diseases, Mayo Clinic, Rochester, Minnesota; [4]Department of Cardiology, Heart Center, Rigshospitalet and Copenhagen University, Copenhagen, Denmark; [5]DC Devices, Boston, Massachusetts; [6]Division of Cardiology, University of Minnesota, Minneapolis, Minnesota; [7]Division of Cardiology, Columbia University, New York, New York and [8]Cardiology Division, Evanston Hospital, Evanston, Illinois.

Manuscript received June 25, 2013; revised manuscript received November 20, 2013; revised manuscript accepted January 3, 2014.

Reprint requests: Daniel Burkhoff, MD, PhD, Division of Cardiology, New York Presbyterian Hospital, 177 Fort Washington Ave, New York, NY 10032. Tel: 201-294-6081. E-mail: db59@columbia.edu

Funding: Supported in part by DC Devices, Boston, Massachusetts, and a program grant (D.M.K.) from the National Health and Medical Research Council of Australia.

See page 219 for disclosure information.

1071-9164/$ - see front matter

http://dx.doi.org/10.1016/j.cardfail.2014.01.005

because these patients as a whole may have different underlying etiologies and varied numbers and severity of comorbid conditions, so that different therapies may be needed to address different patient subgroups. However, regardless of etiology or comorbid conditions, an overarching pathophysiologic mechanism is elevated pulmonary capillary pressure during HF exacerbations and during exertion and increased left atrial size. Accordingly, an approach that directly addresses this hemodynamic abnormality may be therapeutic across disparate patient subgroups.

Detailed characterization of rest and exercise hemodynamics in patients with HF has been performed by several groups[4,5] and most recently in patients with HFpEF.[6–11] Hemodynamic factors that have been suggested to contribute to exercise intolerance in HFpEF include blunted chronotropic response, inability to increase stroke volume, altered oxygen extraction by the periphery and dramatic increases of pulmonary capillary wedge pressure (PCWP) out of proportion to increases of right atrial pressure. To a certain extent, some of these abnormalities are indicative of deconditioning and may be overcome by exercise training[12–14]; however, such improvements do not appear to be linked to improvements in ventricular or vascular properties.[15,16] Despite somewhat different conclusions arrived at in these studies, one common finding is the marked exercise-induced increase of left atrial and pulmonary capillary pressures in HFpEF.

It has recently been proposed that creation of a small permanent opening in the interatrial septum to allow left-to-right shunting of blood could provide a means of limiting left atrial pressure rises, thus potentially improving exercise tolerance and protecting a patient from episodes of acute pulmonary edema. Such a shunt might be especially effective when the pressure gradient between left and right atria is increased, as occurs during exercise in HFpEF patients.

Preclinical evaluation of the hemodynamic effects of such a device is difficult, especially for the case of severe HF with relatively well preserved ejection fraction, because there is no accepted large animal model and, in addition, invasive exercise studies are difficult to conduct in large animal models. To circumvent this problem, we used a computer model to simulate rest and exercise hemodynamics typically encountered in HF. This model has been used before to prospectively predict and/or retrospectively explain different aspects of HF pathophysiology and the effects of treatment.[17–21] For the present simulation, we used hemodynamic data from two published studies of patients with HFpEF[9,10] and then simulated the impact of the presence of an interatrial shunt. The results show the potential benefits, suggest potentially important aspects of patient selection, and point out potential limitations of this approach.

Methods

Patient Population

Rest and exercise hemodynamic data used in the present simulation-based study were previously published by Maeder et al[4] and Borlaug et al.[5] Borlaug et al[5] included 32 patients with EF ≥50% evaluated for effort intolerance and normal resting hemodynamics and B-type natriuretic peptide (BNP), and without significant coronary artery disease, valvular heart disease, hypertrophic or infiltrative cardiomyopathy, constrictive pericarditis, or vascular disease. In that study, patients were also included if PCWP increased to ≥25 mm Hg during exercise. Use of this exercise-PCWP criterion identifies patients who have an unambiguous hemodynamic abnormality contributing to their symptomotology, at least during exercise. Maeder et al studied 14 patients who had EF ≥50%, New York Heart Association functional class II or III signs, and symptoms and objective evidence of impaired exercise capacity but no evidence of myocardial ischemia. To be consistent with the selection criteria of Borlaug et al,[9] we also selected data from 7 of these patients in whom PCWP increased to ≥25 mm Hg during exercise.

Participants in both of these studies underwent detailed echocardiographic and invasive hemodynamic evaluation at rest and during exercise. Right heart catheterization monitoring was performed to assess intracardiac pressures and cardiac output by the thermodilution or direct Fick method. Exercise was performed on a cycle ergometer in the supine position.

Hemodynamic Simulation

We used a previously developed real-time model of the cardiovascular system to simulate hemodynamics at rest and during exercise.[17–21] The equations underlying the model have been provided in detail previously,[17,18] and an overview is provided in Appendix 1. In brief, contractile properties of each heart chamber was modeled as a time-varying elastance, which has been validated for both the ventricles[22] and the atria.[23–29] The systemic and pulmonary vascular beds were modeled by series of resistance and capacitance elements. Parameter values of the model were adjusted by a custom-designed algorithm to fit the average hemodynamic conditions at rest and exercise as defined by the clinical studies noted above.[4,5] Parameters that were varied included right and left ventricular (RV and LV, respectively) chamber systolic properties, vascular resistance, vascular compliance for the systemic vascular beds, and stressed blood volume (which correlates with overall fluid status of the patient). The model was then modified to simulate the presence of a shunt between the right and left atria according to the equation governing instantaneous flow through an orifice as detailed in Appendix 1. Flow = $K \cdot Area \cdot \Delta P$, where Area (in cm^2), ΔP is the pressure gradient across the orifice (in mm Hg), and K = 2.66. The effects of varying shunt sizes up to 12 mm in diameter were also modeled.

Aortic, pulmonary arterial, ventricular, and atrial pressure waveforms, as well as pressure-volume (PV) loops of each of the 4 chambers were constructed for baseline and exercise conditions. The pressure waveforms and pressure-volume loops were also assessed with and without the interatrial shunt.

Results

Although there are limited data available for detailed validation specifically of the atrial simulation aspects of the model used, it is striking that rather detailed aspects of the atrial pressure and volume curves and the impact of acute opening/closing of an atrial septal defect (ASD) can be simulated. For example, see the tracings presented in Figure 1. The left atrial pressure tracing from a patient

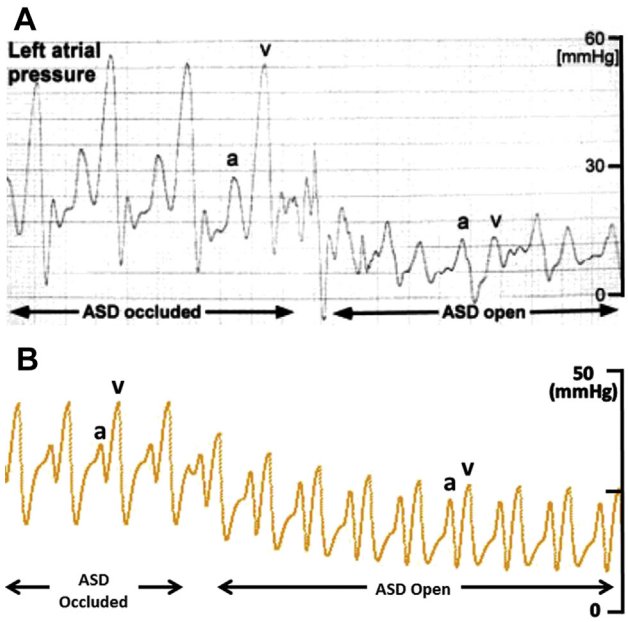

Fig. 1. (A) Left atrial pressure tracing from a patient before and after atrial septal defect (ASD) closure (reproduced from Ewert et al[30]). (B) Left atrial pressure tracings from the simulation with parameters adjusted to achieve a large v-wave (in the absence of any mitral regurgitation) when there is no ASD. Then, an 8-mm-diameter ASD is simulated. Note the qualitative similarity of the real curves to those created in the simulation.

before and after ASD closure (reproduced from Ewert et al[30]) are shown in the top panel. Note that when the shunt is closed during balloon occlusion, mean left atrial pressure is high; there is a small a-wave and a very large v-wave (despite no significant mitral regurgitation), unmasking a stiff LV. When the ASD is opened, the pressure drops, and the a and v waves have similar amplitudes. Left atrial pressure tracings from the simulation with parameters adjusted to achieve a large v-wave (in the absence of any mitral regurgitation) when there is no ASD are shown in the bottom panel. Subsequently, an 8-mm-diameter ASD is simulated. Note the similarity of the characteristics of the real curves to those provided by the simulation.

Resting Versus Exercise Hemodynamics in HFpEF

Demographic characteristics, resting and exercise hemodynamics of the patients included in the 2 clinical studies are summarized in Table 1. Compared with the HF patients studied by Maeder et al,[4] those studied by Borlaug et al[5] were slightly younger, more obese, more often female, with lower NYHA functional class, yet with slightly higher BNP. Despite this, resting and exercise hemodynamics were remarkably similar between the 2 studies. In addition, and importantly, there were no significant differences in resting hemodynamics between the HF and control patients in either study; all values were within normal ranges.

During exercise, the results of the 2 studies were in general agreement in that increases in heart rate and cardiac output during exercise tended to be lower compared with control patients and that increases in arterial, pulmonary, and pulmonary capillary wedge pressures tended to be greater than in control patients.

Table 1. Baseline Characteristics and Comparison of Hemodynamic Parameters at Rest and Exercise in HF Patients

	Clinical Study		Simulation Results	
	Maeder et al[10] (n = 7)	Borlaug et al[9] (n = 32)	Before Shunt	8 mm Shunt
Age (yr)	72	65†		
BSA (m^2)	2.0	NR		
BMI	28†	32†		
% male	64%	28%		
Symptoms				
NYHA II	43%	84%		
NYHA III	57%	16%		
BNP (pg/mL)	40	71		
eGFR (mL/min)	87	86		
Rest hemodynamics				
Heart rate (beats/min)	62	70	65	65
Mean arterial pressure (mm Hg)	100	94	100	90
Mean pulmonary arterial pressure (mm Hg)	19	19	19	17
Pulmonary capillary wedge pressure (mm Hg)	10	11	10	7
Right atrial pressure (mm Hg)	5	5	5	6
Left cardiac output (L/min)	5.3	5.6*	5.3	4.7
Right cardiac output (L/min)	—	—	—	6.1
Shunt flow (L/min)	—	—	—	1.4
Exercise hemodynamics				
Heart rate (beats/min)	106	104	106	106
Mean arterial pressure (mm Hg)	130	125	132	120
Mean pulmonary arterial pressure (mm Hg)	44	43	44	36
Pulmonary capillary wedge pressure (mm Hg)	28	28	28	17
Right atrial pressure (mm Hg)	nr	14	11	13
Left cardiac output (L/min)	9.9	9.8*	9.9	8.8
Right cardiac output (L/min)	9.9	9.9	9.9	11.6
Shunt flow (L/min)	—	—	—	2.8

NR, not reported.
*Assumes a BSA of 2.0.

Simulation of Resting and Exercise Hemodynamics

Parameter values of the simulation were adjusted to match those from the clinical studies as closely as possible. Values of key parameters that varied between rest and exercise are summarized in Table 2, and values of other parameters that remained fixed are summarized in Appendix Table 1. The resulting simulation hemodynamic parameters are summarized in Table 1. As shown, all of the simulated

Table 2. Values of Model Parameters Determined to Simulate Heart Failure Patients at Rest and During Exercise

Parameter	Rest	Exercise
Heart rate (beats/min)	62	106
Stressed blood volume (mL)	880	1,620
Systemic circulation		
C_a (mL/mm Hg)	1.0	0.7
R_a (mm Hg.s/mL)	1.02	0.65
Heart		
LV E_{es} (mm Hg/mL)	2.54	2.70
RV E_{es} (mm Hg/mL)	0.97	1.44

C_a, arterial capacitance; E_{es}, end-systolic elastance; LV, left ventricular; R_a, arterial resistance; RV, right ventricular.
Parameter values not listed here are as summarized in Appendix Table 1.

hemodynamic parameters are very close to those measured in the clinical studies.

Simulated Effects of Interatrial Shunt on Resting Hemodynamics in HF

Figure 2 shows simulated pressure-volume loops at rest for the 4 chambers in the HF patients before (blue) and after (red) introduction of an 8-mm-diameter interatrial shunt. At rest, the shunt decreased LV cardiac output (CO) by 0.6 L/min (from 5.3 to 4.7 L/min) and increased RV CO by 0.8 L/min (from 5.3 to 6.1 L/min). The reason for the slight imbalance between the increased RV output and decreased LV output is that the presence of the shunt changes the filling conditions on the 2 sides of the heart such that a new equilibrium state is reached. The mean flow through the shunt was 1.4 L/min, which corresponds to a Qp/Qs ratio of 1.3. Note that the post-shunt RV output is the sum of the shunt flow plus the LV output (ie, 4.7 + 1.4 = 6.1). The presence of the shunt caused a leftward and downward shift of the LA pressure-volume loop and, conversely, a corresponding rightward and upward shift of the RA pressure-volume loop. However, the rise in mean right atrial pressure was only ~1.0 mm Hg (from 5.0 to 6.0 mm Hg). The decrease in LA volume and pressure resulted in reduced LV filling which, in turn, resulted in leftward and downward shifts in the LV pressure-volume loops (with decreases in LV end-diastolic pressure, end-diastolic volume, stroke volume, and aortic pressure). Conversely, the RV pressure-volume loop shows an increased stroke volume.

As shown in Figure 3 (left), before the shunt there was a significant gradient between RA and LA pressures at rest. However, after the shunt, RA and LA pressures were similar, with only a small gradient throughout the cardiac cycle; however, LA pressure remains greater than RA

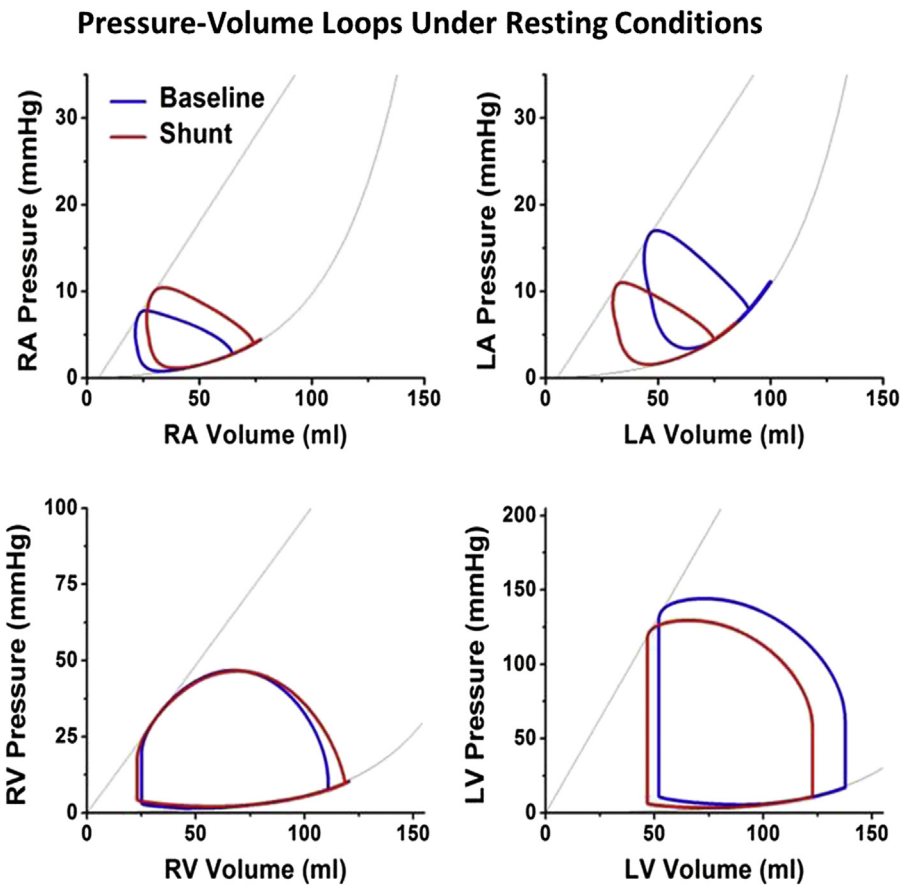

Fig. 2. Pressure-volume loops of the 4 chambers under simulated resting conditions, including the right atrium (RA), right ventricle (RV), left atrium (LA), and left ventricle (LV) in heart failure (HF) patients before (blue) and after (red) simulated introduction of an 8-mm interatrial shunt. At rest, the shunt decreased LV cardiac output by 0.6 L/min and increased RV cardiac output by 0.8 L/min, corresponding to a Qp/Qs ratio of 1.3.

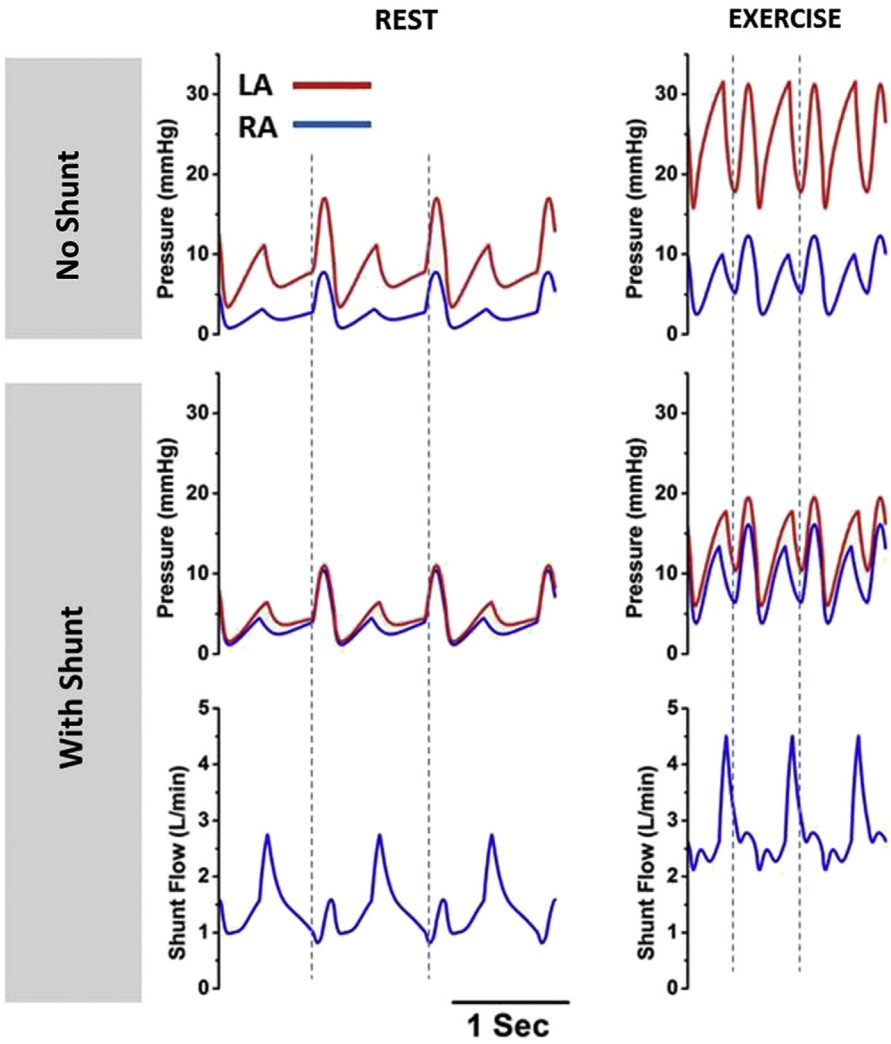

Fig. 3. Left: RA and LA pressure tracings at rest, with typical double-peaked wave forms with each beat (due to the x- and y-descents). Before the shunt (top), there was a small gradient between the LA and RA pressures; this gradient was reduced after the shunt, although the pressure is always greater in the LA than in the RA. Flow pattern through the shunt (middle and bottom) is greatest during atrial diastole when tricuspid and mitral valves are closed and blood is returning to atria from the respective venous systems. Right: RA and LA pressures during exercise. The gradient between the RA and LA is markedly increased and is reduced after the shunt. Shunt flow is increased during exercise, but the pattern is similar to resting conditions. Dashed vertical lines indicate start of each beat. Abbreviations as in Figure 2.

pressure throughout the cycle, and the flow is always from LA to RA. The flow through the shunt (Fig. 3, bottom), is greatest during atrial diastole (ventricular systole) which is the period of rapid venous return to the atria when the atrial-ventricular valves are closed.

Effects of Interatrial Shunt on Exercise Hemodynamics in HFpEF Patients

The pressure-volume loops of the 4 chambers during exercise are shown in Figure 4. Simulated introduction of the interatrial shunt had effects on pressures and volumes that were similar to resting conditions, but the effects were quantitatively greater during exercise. The shunt decreased exercise LV CO by 1.1 L/min (an 11% decrease), and increased RV CO by 1.7 L/min (a 19% increase). The net shunt flow was 2.8 L/min, which corresponds to a Qp/Qs ratio of 1.4.

LA pressure-volume loops were shifted significantly leftward and downward toward lower pressures and volumes, as were the LV pressure-volume loops, with decreases in LV end-diastolic pressure, end-diastolic volume, aortic pressure, and stroke volume (from 93 to 83 mL/beat). Conversely, the RA pressure-volume loops were shifted slightly rightward. The RV pressure-volume loop exhibited increased end-diastolic volume, end-diastolic pressure, and stroke volume. Importantly, although RV CO increased because of the shunt, it is noteworthy that peak exercise pulmonary arterial systolic pressure actually decreased (by ~4 mm Hg, from 81 to 77 mm Hg with mean pressure dropping from 44 to 36 mm Hg) because of the marked reduction in downstream LA pressure.

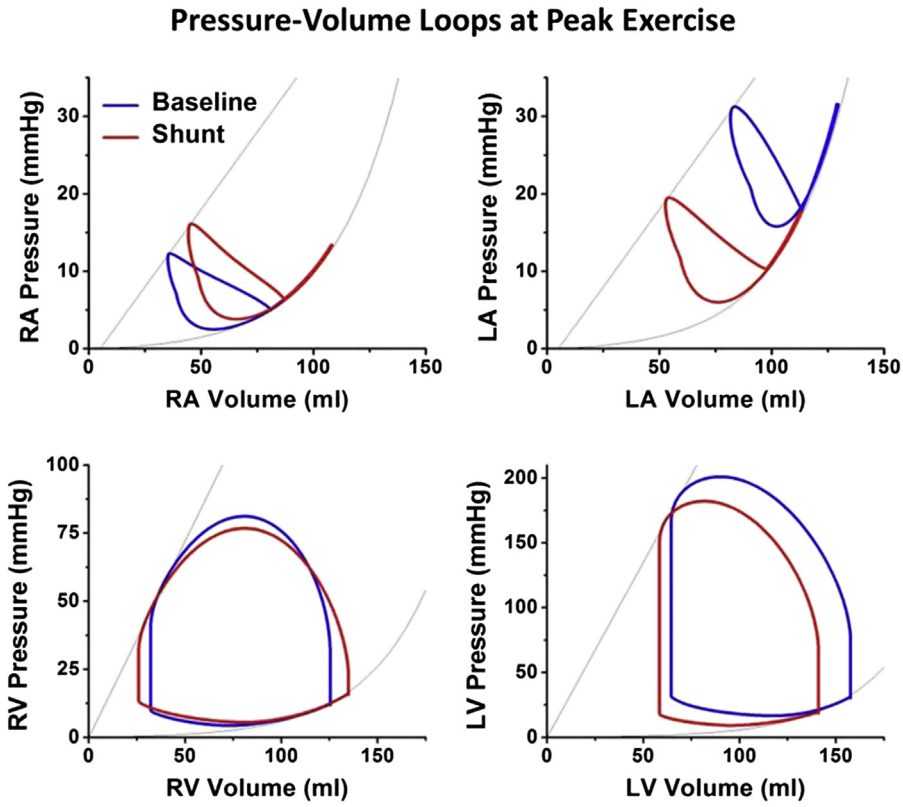

Fig. 4. Exercise pressure-volume loops of the 4 chambers in heart failure patients before (blue) and after (red) simulated introduction of an 8-mm interatrial shunt. Abbreviations as in Figure 2.

The shunt waveform, shown in Figure 3 (bottom right) again peaks in atrial diastole during the phase of rapid venous return. Also shown in Figure 3, although there was a marked pressure gradient between LA and RA at baseline (top), this was largely negated by the shunt (middle right). Importantly, exercise PCWP decreased from 28 to 17 mm Hg with the shunt. As under the resting condition, LA pressure was always greater than RA pressure and flow was always from LA to RA.

Effect of Shunt Diameter

As noted above, the aforementioned simulation results were created with the use of a shunt diameter of 8 mm Hg. Figure 5 summarizes the effect on rest and exercise hemodynamics of varying the shunt diameter from 0 to 12 mm. As expected, shunt flow increases with increasing shunt size at rest and during exercise. Under resting conditions (Fig. 5, left), as shunt flow size is increased, there is a progressive decrease in PCWP and a lesser increase in RA pressure. As shunt flow increases, there is a corresponding increase in RV CO and a decrease in LV CO. All of these effects reach a plateau at a shunt diameter at ∼8−9 mm. During exercise (Fig. 5, right) the effects are significantly more pronounced because of the larger LA-RA pressure gradient under this condition; however, the effect on shunt flow still plateaus at only a slightly larger shunt diameter of ∼10 mm.

Discussion

This study used a cardiovascular simulation to provide insights into the potential effects of an interatrial shunt on rest and exercise hemodynamics in patients with HFpEF. The principal finding is that the interatrial shunt lowers LA pressure and that this effect is particularly pronounced during the marked increase in LA pressure and increased left-to-right atrial pressure gradient during exercise in this patient population. The main consequence of the left-to-right shunt flow is a relatively small (∼10%−15%) but expected decrease in LV forward CO and increase in total RV CO. However, the marked reduction in LA pressure (and pulmonary capillary pressure) could allow patients to exercise longer, potentially resulting in higher heart rates and higher values of CO. In addition, other potential consequences, such as increases in RA pressure and pulmonary arterial pressure are quantitatively smaller. During exercise, when HF symptoms may occur in this patient population, simulated pulmonary arterial systolic pressure actually decreased, despite the increase in RV CO, because the reduction in pulmonary venous pressure was so large. These effects could all be modulated by changing the size of the shunt, but the 8 mm size, with a Qp/Qs ratio of ∼1.3−1.4 (which is similar at rest and during exercise), appeared to be sufficient to reduce LA pressure without major RV overload.

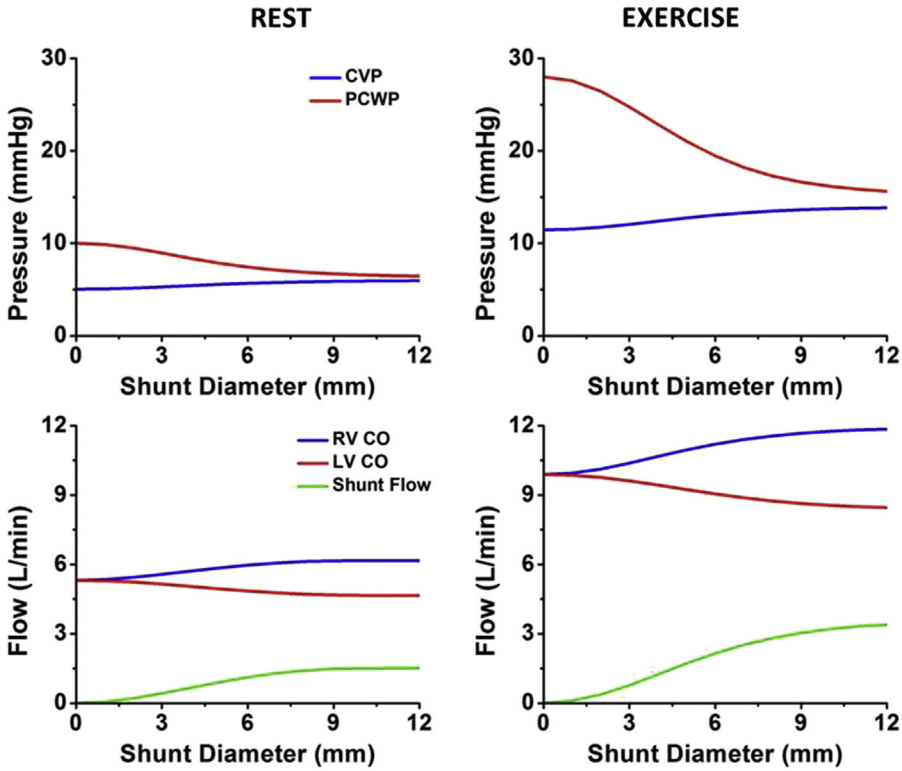

Fig. 5. Effects of varying shunt size from 1 to 12 mm on (left) rest and (right) exercise hemodynamics. Shunt flow increases as shunt size increases. A majority of the hemodynamic effects are seen with shunt sizes of 8−9 mm in diameter. CO, cardiac output; CVP, central venous pressure; PCWP, pulmonary capillary wedge pressure; other abbreviations as in Figure 2.

The theoretical concept of creating an interatrial shunt to treat patients with HF with preserved and mildly reduced ejection fraction and elevated left atrial pressure was based on the key pathophysiologic finding of increased LA pressures with increased LA-to-RA pressure gradient at rest and during exercise. In Lutembacher syndrome,[31] patients with mitral stenosis with an ASD appeared to have fewer symptoms and better outcomes than patients with mitral stenosis who did not have this defect. Furthermore, although closure of congenital ASDs is generally safe, it is long recognized that patients with subclinical LV dysfunction can experience pulmonary edema (sometimes requiring intubation) after surgical[32−34] or interventional[35−38] ASD closure; the pulmonary edema is reversible if the ASD is reopened. As a consequence, some investigators have proposed the use of a fenestrated closure device to achieve partial closure in high-risk patients (eg, those with reduced EF, coronary artery disease, or pulmonary hypertension).[39] More recently, a pilot study using a pressure sensor in the atrial septum that monitors LA pressure in patients with HF was conducted.[40] Daily measurements of LA pressures were used to guide adjustment of diuretic, β-blocker, and angiotensin-converting enzyme inhibitor doses to achieve appropriate LA pressures. The results showed that reductions in mean LA pressures were associated with reductions of adverse outcomes and improvements in EF and NYHA functional class. All of these findings lead to the hypothesis that a device that could reduce and maintain left atrial pressure within a more normal (or at least tolerable) range could have important clinical benefits in patients with HF.

Though derived from a cardiovascular simulation, the present results provide reassurance, given the lack of suitable animal models, that the creation of an interatrial shunt of the size evaluated in our model should not, at least in the acute setting, cause significant elevations of precapillary pulmonary pressures. The reason for this is that the decrease in LA pressure is sufficient to counteract the increase in transpulmonary pressure due to the increase in pulmonary flow. Of course, this hypothesis must be proven in an appropriate clinical trial, but these findings are encouraging.

The present model may also have implications for patient inclusion and exclusion criteria for a clinical trial evaluating the effectiveness of this approach. The data would suggest that the greatest benefit may be achieved in patients who have higher elevations in rest and exercise LA (and pulmonary capillary wedge) pressures and, more precisely, an elevated pressure gradient between left and right atria. Conversely, patients without significantly increased LA pressure and a relatively small gradient between left and right atria may not benefit from such a device or could do worse if there is reversal of shunt direction due to primarily elevated right atrial pressure. However, based on the data from Maeder et al[10] and Borlaug et al,[9] LA pressure should be significantly higher than RA pressure in a majority of these patients, both at rest and during exertion.

Furthermore, given that the shunt is expected to decrease LV CO, the results also suggest that patients in whom reduced CO is the predominant cause of exercise limitation might not benefit as much as those in whom exercise tolerance is limited by a rise in PCWP. Additionally, given the increased flow through the right side of the heart, patients with RV dysfunction may not benefit from this approach.[11]

The clinical data on which the simulation parameters were selected were obtained from patients whose PCWP increased to ≥25 mm Hg during exercise. This criterion followed the suggestion of Borlaug et al[9] and was intended to identify a cohort of patients with unambiguous objective evidence of a hemodynamic abnormality that could contribute to symptomatology during exertion. Accordingly, the results of the present simulation should be considered to apply to this situation only. Patients with lesser degrees of PCWP elevation during exertion might not be anticipated to achieve the same magnitude of hemodynamic benefit as identified in the present analysis. This is important to consider, because it is possible that in some HFpEF patients, inability to increased CO or some other factor may be the exercise-limiting factor without such a significant increase in PCWP.

There are several additional limitations to this study. First, the model parameters were based on average hemodynamics from a small number of patients from 2 studies chosen such that PCWPs were elevated (>25 mm Hg) during exercise. There are undoubtedly patients with less of a pressure gradient between the right and left atria. Therefore, the simulation used in the present study may be primarily helpful in predicting the acute hemodynamic effects in specific patients only if resting and exercise hemodynamics are available. Second, there are many simplifying assumptions in the model, such as lack of interventricular or interatrial interactions and lack of pericardium. Shifts in chamber volumes and changes in pressure gradients between chambers could have important effects on pressure-waveforms and effects of an interatrial shunt. Third, all of the conclusions are based on acute changes, and potential long-term effects of the shunt, when autonomic adaptations can be invoked, can not be assessed in this model. Finally, the acute hemodynamic changes associated with exercise may not lead to an improvement in overall exercise performance, because exercise performance can be affected by many noncardiac factors, such as deconditioning, motivation, and peripheral metabolism.[41,42] Nevertheless respiratory distress may be reduced in these patients. Finally, right and left ventricular properties have been well established to be described by pressure-volume relations and, more generally, by the time-varying elastance model over a very wide range of conditions, including diseased states. Although not as extensively studied, there is ample evidence to support the use of pressure-volume relations and a time-varying elastance model to describe right and left atrial function in health and disease.[23–29] In addition, the pressure-volume loops generated by the model are remarkably similar to those measured directly in health and disease. Nevertheless, the results of the present simulation study should be viewed only as providing a framework for understanding measurements made in the clinical setting.

In summary, we used a computer simulation to gain insight into the effects of an interatrial shunt in patients with HF and reasonably preserved EF. Such a shunt is predicted to yield a Qp/Qs ratio of 1.3−1.4 and would significantly reduce LA pressure, especially during exercise, by allowing blood to flow from the LA to the RA. Considering the magnitude of the Qp/Qs ratio, these effects are predicted not to be associated with significant adverse increases in pulmonary pressures, particularly not during exercise. In the absence of an animal model to evaluate the effects of such a shunt at rest or exercise, these results suggest that this approach is worthy of investigation for patients with HF with elevated LA pressure, especially if EF is preserved or only mildly reduced. There are currently 2 different devices in clinical development to create a device to make a precisely sized interatrial septal defect that will maintain patency for this purpose. The results of the present simulation may provide insights into patient selection criteria and expected magnitude of hemodynamic benefit.

Acknowledgments

The authors are grateful to Dr Micha Maeder for providing raw data from reference 10.

Disclosures

S.K. and D.B. report consulting fees from DC Devices. J.K. and C.M. are employees of DC Devices.

References

1. Owan TE, Hodge DO, Herges RM, Jacobsen SJ, Roger VL, Redfield MM. Trends in prevalence and outcome of heart failure with preserved ejection fraction. N Engl J Med 2006;355:251−9.
2. Bhatia RS, Tu JV, Lee DS, et al. Outcome of heart failure with preserved ejection fraction in a population-based study. N Engl J Med 2006;355:260−9.
3. Steinberg BA, Zhao X, Heidenreich PA, et al. Trends in patients hospitalized with heart failure and preserved left ventricular ejection fraction: prevalence, therapies, and outcomes. Circulation 2012;126:65−75.
4. Kitzman DW, Groban L. Exercise intolerance. Cardiol Clin 2011;29:461−77.
5. Kitzman DW, Groban L. Exercise intolerance. Heart Fail Clin 2008;4:99−115.
6. Borlaug BA, Melenovsky V, Russell SD, et al. Impaired chronotropic and vasodilator reserves limit exercise capacity in patients with heart failure and a preserved ejection fraction. Circulation 2006;114:2138−47.
7. Haykowsky MJ, Brubaker PH, John JM, Stewart KP, Morgan TM, Kitzman DW. Determinants of exercise intolerance in elderly heart failure patients with preserved ejection fraction. J Am Coll Cardiol 2011;58:265−74.

8. Maeder MT, Thompson BR, Htun N, Kaye DM. Hemodynamic determinants of the abnormal cardiopulmonary exercise response in heart failure with preserved left ventricular ejection fraction. J Card Fail 2012;18:702−10.
9. Borlaug BA, Nishimura RA, Sorajja P, Lam CS, Redfield MM. Exercise hemodynamics enhance diagnosis of early heart failure with preserved ejection fraction. Circ Heart Fail 2010;3:588−95.
10. Maeder MT, Thompson BR, Brunner−la Rocca HP, Kaye DM. Hemodynamic basis of exercise limitation in patients with heart failure and normal ejection fraction. J Am Coll Cardiol 2010;56:855−63.
11. Abudiab MM, Redfield MM, Melenovsky V, et al. Cardiac output response to exercise in relation to metabolic demand in heart failure with preserved ejection fraction. Eur J Heart Fail 2013;15:776−85.
12. Kitzman DW, Brubaker PH, Morgan TM, Stewart KP, Little WC. Exercise training in older patients with heart failure and preserved ejection fraction: a randomized, controlled, single-blind trial. Circ Heart Fail 2010;3:659−67.
13. Edelmann F, Gelbrich G, Dungen HD, et al. Exercise training improves exercise capacity and diastolic function in patients with heart failure with preserved ejection fraction: results of the Ex-DHF (Exercise Training in Diastolic Heart Failure) pilot study. J Am Coll Cardiol 2011;58:1780−91.
14. Haykowsky MJ, Brubaker PH, Stewart KP, Morgan TM, Eggebeen J, Kitzman DW. Effect of endurance training on the determinants of peak exercise oxygen consumption in elderly patients with stable compensated heart failure and preserved ejection fraction. J Am Coll Cardiol 2012;60:120−8.
15. Fujimoto N, Prasad A, Hastings JL, et al. Cardiovascular effects of 1 year of progressive endurance exercise training in patients with heart failure with preserved ejection fraction. Am Heart J 2012;164:869−77.
16. Kitzman DW, Brubaker PH, Herrington DM, et al. Effect of endurance exercise training on endothelial function and arterial stiffness in older patients with heart failure and preserved ejection fraction: a randomized, controlled, single-blind trial. J Am Coll Cardiol 2013;62:584−92.
17. Santamore WP, Burkhoff D. Hemodynamic consequences of ventricular interaction as assessed by model analysis. Am J Physiol 1991; 260(HCP 29):H146−57.
18. Burkhoff D, Tyberg JV. Why does pulmonary venous pressure rise following the onset of left ventricular dysfunction: a theoretical analysis. Am J Physiol 1993;265(HCP 34):H1819−28.
19. Dickstein ML, Burkhoff D. A theoretic analysis of the effect of pulmonary vasodilation on pulmonary venous pressure: implications for inhaled nitric oxide therapy. J Heart Lung Transplant 1996;15:715−21.
20. Hay I, Rich J, Ferber P, Burkhoff D, Maurer MS. The role of impaired myocardial relaxation in the production of elevated left ventricular filling pressure. Am J Physiol Heart Circ Physiol 2004;288:H1203−8.
21. Morley D, Litwak K, Ferber P, et al. Hemodynamic effects of partial ventricular support in chronic heart failure: results of simulation validated with in vivo data. J Thorac Cardiovasc Surg 2007;133:21−8.
22. Burkhoff D, Mirsky I, Suga H. Assessment of systolic and diastolic ventricular properties via pressure-volume analysis: a guide for clinical, translational, and basic researchers. Am J Physiol Heart Circ Physiol 2005;289:H501−12.
23. Alexander J Jr, Sunagawa K, Chang N, Sagawa K. Instantaneous pressure-volume reltation of the ejecting canine left atrium. Circ Res 1987;61:209−19.
24. Weimar T, Watanabe Y, Kazui T, et al. Differential impact of short periods of rapid atrial pacing on left and right atrial mechanical function. Am J Physiol Heart Circ Physiol 2012;302:H2583−91.
25. Hoit BD, Shao Y, Gabel M, Walsh RA. In vivo assessment of left atrial contractile performance in normal and pathological conditions using a time-varying elastance model. Circulation 1994;89:1829−38.
26. Lau VK, Sagawa K, Suga H. Instantaneous pressure-volume relationship of right atrium during isovolumic contraction in canine heart. Am J Physiol 1979;236:H672−9.
27. Dernellis JM, Stefanadis CI, Zacharoulis AA, Toutouzas PK. Left atrial mechanical adaptation to long-standing hemodynamic loads based on pressure-volume relations. Am J Cardiol 1998;81: 1138−43.
28. Hoit BD, Shao Y, Gabel M, Walsh RA. Left atrial mechanical and biochemical adaptation to pacing induced heart failure. Cardiovasc Res 1995;29:469−74.
29. Ferguson JJ III, Miller MJ, Aroesty JM, Sahagian P, Grossman W, McKay RG. Assessment of right atrial pressure-volume relations in patients with and without an atrial septal defect. J Am Coll Cardiol 1989;13:630−6.
30. Ewert P, Berger F, Nagdyman N, et al. Masked Left Ventricular Restriction in Elderly Patients With Atrial Septal Defects: A Contraindication for Closure? Cathet Cardiovasc Intervent 2001;52: 177−80.
31. Lutembacher R. De la stenose mitrale avec communication interauriculaier. Arch Mal Coeur Vaiss 1916;9:237−60.
32. Beyer J. Atrial septal defect: acute left heart failure after surgical closure. Ann Thorac Surg 1978;25:36−43.
33. Beyer J, Brunner L, Hugel W, et al. [Acute left heart failure following repair of atrial septal defects. Its treatment by reopening]. Thoraxchir Vask Chir 1975;23:346−9.
34. Davies H, Oliver GC, Rappoport WJ, Gazetopoulos N. Abnormal left heart function after operation for atrial septal defect. Br Heart J 1970; 32:747−53.
35. Ewert P, Berger F, Nagdyman N, et al. Masked left ventricular restriction in elderly patients with atrial septal defects: a contraindication for closure? Catheter Cardiovasc Interv 2001;52:177−80.
36. Ewert P, Berger F, Nagdyman N, Kretschmar O, Lange PE. [Acute left heart failure after interventional occlusion of an atrial septal defect]. Z Kardiol 2001;90:362−6.
37. Tomai F, Gaspardone A, Papa M, Polisca P. Acute left ventricular failure after transcatheter closure of a secundum atrial septal defect in a patient with coronary artery disease: a critical reappraisal. Catheter Cardiovasc Interv 2002;55:97−9.
38. Matsubara T, Yamazoe M, Koike T, Izumi T, Shibata A. A case of atrial septal defect combined with hypertension and left ventricular hypertrophy. Left ventricular failure induced by balloon occlusion and the effect of nifedipine. Jpn Heart J 1989;30:103−7.
39. Schneider HE, Jux C, Kriebel T, Paul T. Fate of a modified fenestration of atrial septal occluder device after transcatheter closure of atrial septal defects in elderly patients. J Interv Cardiol 2011;24: 485−90.
40. Ritzema J, Troughton R, Melton I, et al. Physician-directed patient self-management of left atrial pressure in advanced chronic heart failure. Circulation 2010;121:1086−95.
41. Kitzman DW, Haykowsky MJ. Invited editorial commentary for American Heart Journal mechanisms of exercise training in heart failure with preserved ejection fraction: central disappointment and peripheral promise. Am Heart J 2012;164:807−9.
42. Kraemer MD, Kubo SH, Rector TS, Brunsvold N, Bank AJ. Pulmonary and peripheral vascular factors are important determinants of peak exercise oxygen uptake in patients with heart failure. J Am Coll Cardiol 1993;21:641−8.
43. Guyton AC, Lindsey AW, Abernathy B, Richardson T. Venous return at various right atrial pressures and the normal venous retrun curve. Am J Physiol (Heart Circ Physiol) 1957;189:609−15.
44. Guyton AC, Armstrong GG, Chipley PL. Pressure-volume curves of the arterial and venous systems in live dogs. Am J Physiol (Heart Circ Physiol) 1956;184:253−8.
45. Milnor WR. Hemodynamics. Baltimore: Williams and Wilkins; 1982. p. 1.
46. Sagawa K, Maughan WL, Suga H, Sunagawa K. Cardiac contraction and the pressure-volume relationship. Oxford: Oxford University Press; 1988. p. 1.

Appendix 1

The cardiovascular system was modeled as shown by the electrical analog in Appendix Figure 1. The details of this model are provided elsewhere[17,18] and are discussed here in brief. Ventricular and atrial pumping characteristics were represented by modifications of the time-varying elastance [(E(t)] theory of chamber contraction, which relates instantaneous ventricular pressure [P(t)] to instantaneous ventricular volume [V(t)]. For each chamber:

$$P(t) = P_{ed}(V) + e(t)[P_{es}(V) - P_{ed}(V)]$$

In which:

$$P_{ed}(V) = \beta\left(e^{\alpha(V-V_o)} - 1\right)$$

$$P_{es}(V) = E_{es}(V - V_o)$$

and

$$e(t) = \tfrac{1}{2}\{\sin[(\pi/T_{max})t - \pi/2] + 1\} \quad 0 < t \leq 3/2T_{max}$$

$$\tfrac{1}{2}e^{-(t-3T_{max}/2)/\tau} \quad t > 3T_{max}/2$$

where $P_{ed}(V)$ is end-diastolic pressure as a function of volume, $P_{es}(V)$ is end-systolic pressure as a function of volume, E_{es} is end-systolic elastance, V_o is the volume axis intercept of the end-systolic pressure-volume relationship, α and β are parameters of the end-diastolic pressure-volume relationship, T_{max} is the point of maximal chamber elastance, τ is the time constant of relaxation, and t is the time during the cardiac cycle.

The systemic and pulmonary circuits are each modeled by lumped venous and arterial capacitances (C_v and C_a, respectively), a proximal resistance (R_c, also commonly called characteristic impedance) which relates to the stiffness of the proximal aorta or pulmonary artery, a lumped arterial resistance (R_a), and a resistance to return of blood from the venous capacitance to the heart (R_v, which is similar, though not identical, to Guyton's resistance to venous return[43]). The heart valves permit flow in only 1 direction through the circuit.

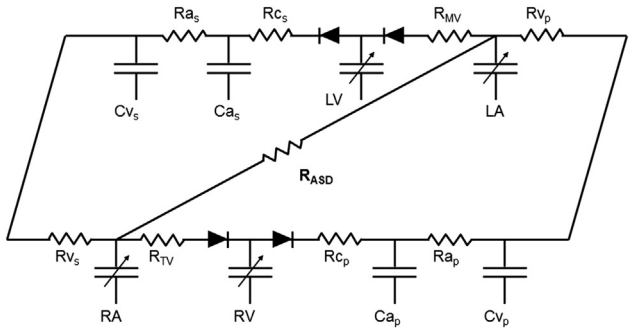

Appendix Figure 1. Electrical analog of the circulation showing heart chambers represented by time-varying elastances and the vascular systemts represented by series of resistance and capacitance elements. Abbreviations as in Appendix Table 1.

The total blood volume (V_{tot}) contained within each of the capacitive compartments is divided functionally into 2 pools: the unstressed blood volume (Vol_{unstr}) and the stressed blood volume (Vol_{str}). Vol_{unstr} is defined as the maximum volume of blood that can be placed within a vascular compartment without raising its pressure above 0 mm Hg. The blood volume within the vascular compartment in excess of Vol_{unstr} is Vol_{str}, so that $V_{tot} = V_{unstr} + V_{str}$. The unstressed volume of the entire vascular system is equal to the sum of Vol_{unstr} of all of the capacitive compartments; similarly, the total-body stressed volume equals the sum of Vol_{str} for all compartments.[44] The pressure within each compartment rises linearly with Vol_{str} in relation to the compliance (C): $P = Vol_{str}/C$.

The normal value of each parameter of the model was set to be appropriate for a 70–75 kg man (body surface area 1.9 m^2). These values, adapted from values in the literature,[17,23,45,46] are listed in Appendix Table 1. Values used to simulate patients with HFpEF are summarized in Table 2 of the main text.

Finally, an interatrial shunt was modeled by a connection between right and left atria through which instantaneous flow was determined by the equation governing flow through an orifice:

$$\text{Flow} = K \cdot \text{Area} \cdot \Delta P$$

where Area is in cm^2, ΔP is the pressure gradient across the orifice (in mm Hg), and K = 2.66.

Appendix Table 1. Baseline Parameter Values Not Adjusted in Simulation Model

Parameter Group/Name	Symbol	Units	Value			
AV Delay	AVD	ms	160			
Heart			RA	RV	LA	LV
Volume axis intercept	V_o	mL	5	0	5	0
Scaling factor for EDPVR	β	mm Hg	0.44	0.34	0.44	0.34
Exponent for EDPVR	α	mL^{-1}	0.044	0.034	0.044	0.034
Time to end-systole	T_{max}	ms	125	200	125	200
Time constant of relaxation	T	ms	25	50	25	50
AV valve resistance	R_{av}	mm Hg·s/mL	0.0025		0.0025	
Circulation			Pulmonary			Systemic
Characteristic impedance	R_c	mm Hg·s/mL	0.045			0.045
Arterial resistance	Ra	mm Hg·s/mL	0.052			
Venous resistance	R_v	mm Hg·s/mL	0.025			0.025
Arterial compliance	C_a	mL/mm Hg	7			1.0
Venous compliance	C_v	mL/mm Hg	4			70

AV, atrioventricular; EDPVR, end-diastolic pressure-volume relationship.